Thermal Stability and Recrystallization of Nanocrystalline Ti Produced by Cryogenic Milling

FUSHENG SUN, ALEJANDRO ZÚÑIGA, PAULA ROJAS, and ENRIQUE J. LAVERNIA

The grain growth, thermal stability, and recrystallization behavior of a cryomilled Ti alloy with a grain size of about 21.2 nm were examined using differential scanning calorimetry, X-ray diffraction, and transmission electron microscopy. Isochronal heat treatments at different temperatures were applied to study the thermal stability and recrystallization behavior of this alloy system. The average grain size increased from 20 to 80 nm in the temperature range of 200 °C to 350 °C, and then significantly decreased to 15 nm during annealing at 400 °C to 450 °C. This phenomenon was rationalized on the basis of a recrystallization mechanism. When the annealing temperature increased from 450 °C to 720 °C, the grain size increased slightly from 15.2 to 27.5 nm. In addition, the isothermal grain growth behavior in this alloy was investigated in the temperature range of 150 °C to 720 °C, and the resulting grain growth activation energy was analyzed to rationalize the underlying grain growth mechanisms. An interesting scientific question that arises from the present work is whether a decrease in grain size can be obtained in nanocrystalline (nc) materials *via* a recrystallization mechanism. The present results show that indeed a smaller grain size is obtained after annealing at elevated temperatures (500 °C to 720 °C) in cryomilled nc Ti, and the experimental results are explained on the basis of a recrystallization mechanism.

I. INTRODUCTION

NANOCRYSTALLINE (nc) materials are of interest due to their unique combinations of physical and mechanical properties.[1–4] The issue of thermal stability in nc materials is important for two primary reasons. First, because on the basis of a Gibb's free energy argument, such fine grains may be metastable, and hence prone to coarsening with a low energy threshold. Second, engineering applications require the consolidation of nc materials, which typically involves exposure to temperature and pressure. Inspection of the scientific literature reveals that the goal of maintaining a stable nc structure through consolidation at elevated temperatures has thus far remained elusive, with few exceptions reported. A number of investigations on the thermal stability of nc materials have been carried out, and the findings reveal that in pure metals, significant grain growth occurs at room temperature, *e.g.*, Sn, Pb, Al, Mg,[5] Cu, and Pd.[6,7] This is particularly noteworthy in the case of Pd since room temperature corresponds to a homologous temperature of only 0.16 T_M. In the case of multicomponent systems, however, it is possible to attain a degree of thermal stability *via* a reduction in grain boundary mobility of the nc grains. This is accomplished, primarily, through the introduction of fine dispersed phases and grain boundary segregation. Recent interest in cryomilling (*e.g.*, milling in a liquid nitrogen media) stems from reports that it is possible to increase the stability of nc grains in metallic systems such as Al, Zn, Ni, and Fe, by introducing a dispersion of nanometer nitride phases.[8–13]

The presence of grain boundary segregation,[14,15,16] solute drag,[17] impurities,[18] second-phase drag,[19] pore drag,[20] and chemical ordering[21,22] can improve the thermal stability of nc materials *via* a drag-force mechanism on the grain boundaries. In related studies, several researchers have examined the thermal stability of nc powders generated by mechanical alloying or mechanical milling.[11,13,23–25] Significant stabilization of nc grain structures was reported, and a generalized criterion appears to be that they are multicomponent, *i.e.*, either containing impurities or alloying elements. For example, the grain size in a 5083 Al alloy reportedly remained in the 30- to 35-nm range, despite a thermal exposure equivalent to 0.61 T_m. This behavior was attributed to the presence of AlN and Al_2O_3 particles.[11] In related studies, the enhanced thermal stability of a cryomilled Fe-10Al alloy was attributed to the formation of Al_2O_3 or oxynitride phases.[13]

The kinetics of grain growth in nc materials has been investigated, and available findings suggest that it cannot be described by a simple power law of the type applicable to grain growth in highly pure, coarse-grained polycrystalline materials.[23,24] For general purposes, an empirical relationship allowing the description of isothermal grain growth has been widely used in the form of[26]

$$D^n - D_0^n = kt \qquad [1]$$

where D is the mean grain size at annealing time t, D_0 the initial grain size, n the empirical time exponent ($n \geq 2$), and k a constant. The practically unavoidable presence of impurities, solute atoms, or second-phase particles in nc samples gives rise to significant retarding forces on the grain-boundary mobility such that the long-time grain growth shows an eventual stagnation at a limiting grain size.

FUSHENG SUN, formerly Postdoctoral Researcher with the Department of Chemical Engineering and Materials Science, University of California, is Senior Technical Specialist, RTI International Metals, Niles, OH. ALEJANDRO ZÚÑIGA, formerly Graduate Student with the Department of Chemical Engineering and Materials Science, University of California, is Instructor, Departamento de Ingenieria Mecánica, Universidad de Chile. PAULA ROJAS, formerly Postdoctoral Researcher with the Department of Chemical Engineering and Materials Science, University of California, is Postdoctoral Researcher, Instituto de Física, Pontificia Universidad Católica de Valparaiso, Chile. ENRIQUE J. LAVERNIA, Dean, is with the College of Engineering, Department of Chemical Engineering and Materials Science, University of California, Davis, CA 95616. Contact e-mail: lavernia@ucdavis.edu

Manuscript submitted November 2, 2005.

Burke[27] introduced a maximum grain size D_M to account for the pinning effect of a second phase (a constant pinning force). The grain growth can then be expressed using the following equation:

$$\frac{D_0 - D}{D_M} + \ln\left(\frac{D_M - D_0}{D_M - D}\right) = \frac{k}{D_M^2} t \qquad [2]$$

where D_0 is the initial grain size and k a constant. As the grain-boundary area decreases, the concentration of solute or impurity atoms segregated to the boundaries is expected to increase rapidly, introducing a grain-size dependence of the retarding force on the boundary migration. Invoking a linear dependence of the grain boundary pinning force on the grain size, Michels *et al.* obtained the following grain growth equation:[28]

$$\frac{D^2 - D_M^2}{D_0^2 - D_M^2} = \exp\left(-\frac{2kt}{D_M^2}\right) \qquad [3]$$

The isochronal variation of grain size at different temperatures in nc materials has been extensively investigated in Al,[9,12,29] Zn,[10] Ni,[8,30] Cu,[31] Fe,[23] and RuAl.[24] The variation of grain size in these nc materials showed positive temperature dependence in a wide range of annealing temperatures. At lower temperatures, annealing of the nc samples led to recovery of the microstructure (strain relaxation and grain coalescence), while at higher temperatures, annealing of the nc samples resulted in recrystallization and a rapid increase in the average grain size. The onset temperature of the grain growth process is dependent on the microstrain introduced during milling or deformation.[23,29]

In contrast, coarse-grain polycrystalline materials showed an optimized annealing temperature where a smaller final grain size can be obtained through a recrystallization process.[32] Recrystallization is considered to be a nucleation and growth phenomenon, controlled by thermally activated processes, whose driving force is provided by the stored energy of deformation. The recrystallized grain size depends primarily on the amount of deformation. The magnitude of the nucleation rate is more affected by strain than the growth rate. Therefore, a higher strain will provide more nuclei per unit volume and hence a smaller final grain size.

It is therefore of scientific and technological interest to investigate the thermal stability and recrystallization behavior of nc materials. One important scientific question in this context is whether a smaller grain size can be obtained in nc materials at a higher annealing temperature through a recrystallization process or if the grain growth in nc materials merely involves the positive temperature dependence. If the first case is true, a new class of nc materials would be designed and synthesized, and their thermal stability can be further enhanced through the recrystallization process.

The current study was undertaken in an effort to understand the grain growth, thermal stability, and recrystallization behavior during annealing of an nc Ti powder produced by ball milling at a cryogenic temperature. The isochronal heat treatment at different temperatures was applied to study the thermal stability and recrystallization behavior of this alloy. In addition, the isothermal grain growth in this alloy has been investigated in a temperature range of 150 °C to 720 °C, and the resulting activation energy for grain growth has been analyzed to explain the underlying grain growth mechanisms. Notably, our experimental results revealed that a smaller average grain size (equiaxed grains) could be obtained after annealing at higher temperatures (500 °C to 720 °C) in the cryomilled nc Ti through a recrystallization process.

II. EXPERIMENTAL PROCEDURES

Elemental Ti powders with 99.9 pct purity were used as the starting material. The nc samples were produced by ball milling the Ti powders under liquid nitrogen. The milling was carried out in a modified Union Process attritor with a stainless steel vial and balls with a rate of 500 rpm. The ball-to-powder ratio was 30:1. After 6 hours of milling, the powder was removed from the attritor and stored in a glove box at room temperature. The composition of the milled Ti powder was obtained by chemical analysis conducted at a commercial laboratory (LECO Inc., St. Joseph, MI) and is shown in Table I.

The isochronal annealing (2 and 60 minutes) of the milled Ti samples was performed at a temperature range of 150 °C to 720 °C with the aim to determine the temperature dependence of the average grain size. In addition, the isothermal annealing of the milled Ti powders was carried out for 0.02, 0.1, 2, 20, 60, 180, and 300 minutes at different temperatures in an attempt to understand the grain growth behavior and the underlying mechanisms. The annealing was performed under a flowing Ar atmosphere in a Perkin-Elmer (Wellesley, MA) DSC-7 with the temperature calibrated using pure In and Zn standards. The powder samples were sealed in a Cu pan and heated to the given temperatures at a rate of 80 °C/min, and then rapidly cooled to room temperature.

X-ray diffraction (XRD) measurements were conducted using a Scintag (Scintag Inc., Cupertino, CA) XDS 2000 X-ray diffractometer equipped with a graphite monochromater using Cu K_α ($\lambda = 0.15406$ nm) radiation. A low scanning rate of 0.6 deg/min and a step time of 2 seconds were used for phase identification and grain size measurements. Determination of grain size and microstrain of the as-milled and annealed Ti powders was performed using the single line approximation (SLA) analysis, developed by Keijser *et al.*[33] The experimentally measured line profile, h, is actually a combination of the structurally broadened profile, f, and the standard profile, g. The instrumental broadening (the standard profile g) was corrected using an annealed (200 °C/3 h) Ti sample. After correction of the instrumental broadening, the integral widths of β_C^f and β_G^f are given by

$$\beta_C^f = \beta_C^h - \beta_C^G \text{ and } (\beta_G^f)^2 = (\beta_G^h)^2 - (\beta_G^g)^2 \qquad [4]$$

where β_C^f and β_G^f are the constituent Cauchy and Gaussian components, respectively. The constituent Cauchy and

Table I. Chemical Analysis of the Cryomilled Ti Powder

Ti	O, Wt Pct	N, Wt Pct	C, Wt Pct	H, ppm	Fe, Wt Pct
Matrix	0.501	2.17	0.0183	300.5	0.083

Gaussian components can be calculated from the values of β and the 2 w/β (where 2 w is the full-width at half-maximum of the XRD peak) using the following empirical equations:[33]

$$\beta_C = \beta \cdot \left[2.0207 - 0.4803 \cdot \left(\frac{2w}{\beta} \right) - 1.7756 \cdot \left(\frac{2w}{\beta} \right)^2 \right] \quad [5]$$

$$\beta_G = \beta \cdot \left[0.6420 + 1.4187 \cdot \left\langle \left(\frac{2w}{\beta} \right) - \frac{2}{\pi} \right\rangle^{1/2} - 2.2043 \cdot \left(\frac{2w}{\beta} \right) + 1.8706 \cdot \left(\frac{2w}{\beta} \right)^2 \right] \quad [6]$$

Approximating the grain size broadening profiles by a Cauchy function and strain broadening profiles by a Gaussian function, the grain size (D) and the strain (e) can be estimated from each diffraction peak with diffraction angle (θ) by

$$D = \frac{k\lambda}{\beta_C^f \cos\theta} \quad [7]$$

$$e = \frac{\beta_G^f}{4 \tan\theta} \quad [8]$$

The six strongest XRD peaks in the Ti samples were employed to measure the grain size and microstrain.

The TEM microscopy studies were carried out using a PHILIPS* CM20 microscope operated at 200 kV. The annealed Ti powders were mixed in G-1 epoxy (Gatan Inc., Warrendale, PA) to form a small disk by curing the epoxy-powder mixture at room temperature. The samples were mechanically polished, dimpled, and ion milled.

*PHILIPS is a trademark of Philips Electronic Instruments, Mahwah, NJ.

III. RESULTS

A. *Thermal Stability*

The XRD peaks of the as-received, as-cryomilled, and as-annealed Ti powders were measured in the 2θ range from 25 to 90 deg. In the as-cryomilled and as-annealed nc Ti samples, only hcp α-Ti was identified. In order to clearly show the peak broadening phenomenon after annealing, the XRD patterns in the diffraction range of 33 to 45 deg corresponding to the as-cryomilled (6 hours) and as-annealed (350 °C and 675 °C for 60 minutes) samples are shown in Figure 1. The lattice parameters of the as-cryomilled nc Ti powder are $a = 0.2957$ nm and $c = 0.4694$ nm, slightly larger than those of the as-received Ti powder ($a = 0.2954$ nm and $c = 0.4687$ nm). According to the XRD line broadening analysis (using six Bragg reflections), we obtained an average grain size of 21.2 nm and a mean microstrain of about 0.52 pct. These values compare relatively well with those of 0.1 to 0.6 pct strain found in cryomilled Ni and Fe.[23,34] In comparison to other deformation processes, cryomilling induces a higher residual strain due to a lower recovery rate caused by the lower processing temperature.[35] For the sample annealed at 350 °C for 60 minutes, a sharpening of the diffraction peaks is observed, indicating the presence of grain growth during annealing. However, annealing at higher temperatures (450 °C to 720 °C) for 60 minutes led to broadening of the diffraction peaks, indicating that recrystallization occurred at higher temperatures. A distinct shift of the diffraction peaks from the as-cryomilled nc Ti powder toward lower diffraction angles was observed in the XRD pattern of the as-annealed powders. The lattice parameters of the annealed samples are $a = 0.2959$ nm and $c = 0.4742$ nm, significantly larger than those of the as-cryomilled nc Ti. Assuming that the lattice expansion can be attributed solely to dissolved N atoms, the lattice parameters can be estimated based on the data in Reference 36. The effect of the N atoms on the recrystallization will be discussed in Section IV–A.

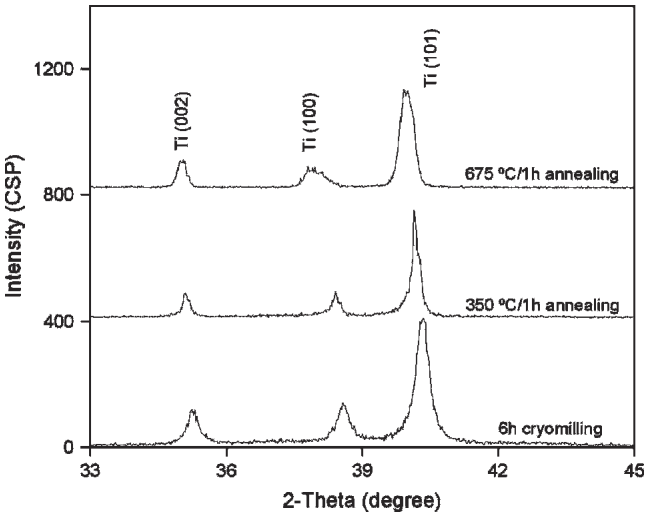

Fig. 1—XRD pattern for the 6h-cryomilled and annealed Ti powders.

In order to explore the thermal stability of the nc Ti powder, various samples annealed at different temperatures were analyzed by means of quantitative XRD to determine the grain size and microstrain. The variations of the average grain size and microstrain *vs* the annealing temperature for the two different annealing times (2 and 60 minutes) are shown in Figure 2. From the XRD results shown in Figure 2(a), there was no obvious grain growth below 150 °C. In the temperature range from 200 °C to 350 °C, an increase in the average grain size from 20 to 80 nm was observed. With a further increase of the annealing temperature, a significant drop of the average grain size (to approximately 15.2 nm) was observed during annealing at 400 °C to 450 °C, which is proposed to occur due to a recrystallization process. Finally, when the annealing temperature increased from 450 °C to 720 °C, the grain size increased from 15.2 to 27.5 nm, indicating that no significant grain growth occurs between 450 °C and 720 °C.

The mean microstrain (e) in the nc Ti samples as a function of the annealing temperature is shown in Figure 2(b). After annealing at temperatures ranging from 150 °C to 350 °C, the microstrain (e) decreased from 0.52 to 0.11 pct. When the temperature is increased to 400 °C to

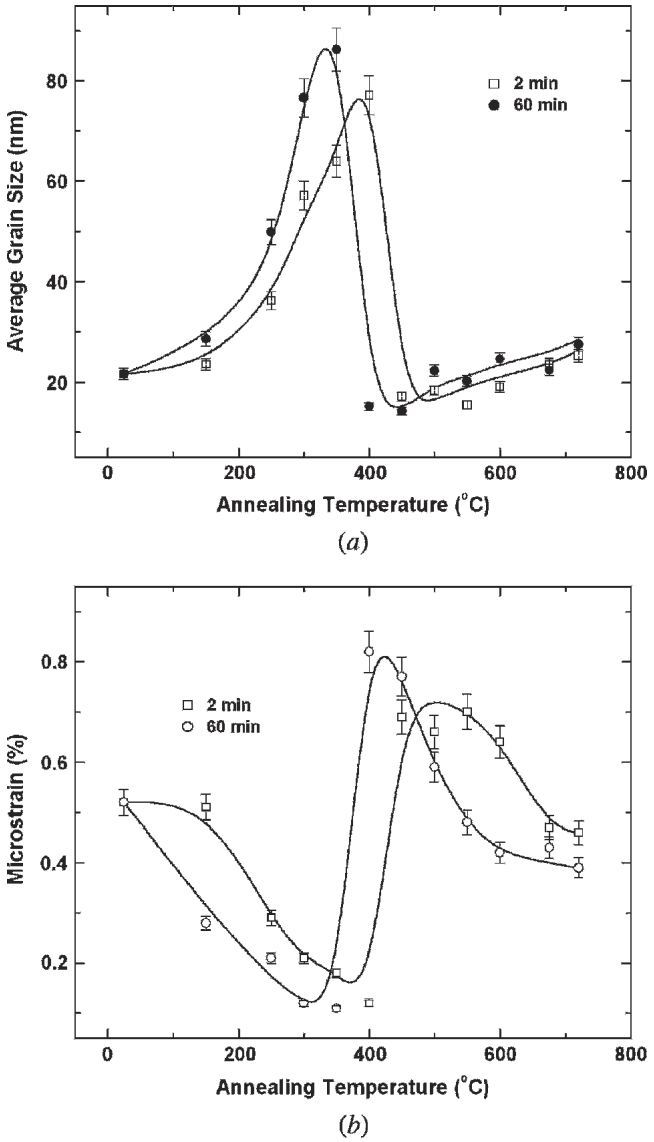

Fig. 2—(*a*) Grain size and (*b*) microstrain *vs* annealing temperature for two annealing times (2 and 60 min).

450 °C, the microstrain increased significantly to about 0.77 to 0.86 pct as a result of recrystallization. However, the microstrain decreased slowly as the annealing temperature increased from 450 °C to 720 °C. This observation correlates with the analysis of grain growth presented in Figure 2(a).

Microstructural characterization by means of TEM observations indicated that the grain sizes obtained from XRD are generally similar to those observed in the TEM images. For example, the bright-field and dark-field images in Figures 3(a) and (b) show the as-6h-cryomilled powder with a grain size of about 21.2 nm, while the dark-field image in Figure 3(c) shows the sample annealed at 675 °C for 60 minutes with a grain size of about 22.4 nm, as a result of recrystallization. Figure 3(d) shows the selected area diffraction pattern (SADP) after recrystallization (corresponding to Figure 3(c)), in which only hcp Ti SADP rings were observed and no TiN phase was detected. The grain size distributions as cryomilled and as annealed at 675 °C for 60 minutes are shown in Table II.

B. *Grain Growth at Low Temperatures (150 °C to 350 °C)*

The isothermal grain growth kinetics for the as-cryomilled nc Ti powder in the annealing temperature range from 150 °C to 350 °C are plotted in Figure 4. Grain growth stagnated after a certain annealing time at all temperatures in Figure 4(a), while microstrain decreased rapidly after the first period of annealing and then maintained a certain value, as shown in Figure 4(b). The higher the temperature, the lower the microstrain achieved after the first period of annealing. At each annealing temperature, the experimental data of grain sizes were fitted to Eq. [3] by using a linear curve fit computer program to determine the best-fit values for the parameters k and D_M (shown in Table III). The solid lines in Figure 4(a) are the fitted curves.

We make the usual assumption that the rate constant parameter k in Eq. [3] has an Arrhenius dependence on temperature:[28]

$$k = k_0 \exp\left[-\frac{E}{k_B T}\right] \qquad [9]$$

where E is the apparent activation energy, T the absolute temperature, k_B the Boltzmann constant, and k_0 a constant. Based on the variation of the rate constant k *vs* the reciprocal annealing temperature (Figure 5), the activation energy E for grain growth may be calculated using Eq. [9]. The resultant activation energy for isothermal grain growth is 62.1 kJ/mol, much lower than the activation energy for lattice self-diffusion of Ti (169.1 kJ/mol) and lattice diffusion of N in Ti (224 kJ/mol).[37] Two diffusion mechanisms may be considered for the grain growth process: diffusion through the lattice or via grain boundaries. Grain boundary diffusion becomes the dominant mechanism when the ratio of grain boundary diffusivity D_{gb} and bulk diffusivity D_v is greater than the ratio of grain size, d, to boundary width, δ (*i.e.*, $D_{gb}/D_v > d/\delta$), especially at lower temperatures.[38] In this study, the average grain sizes of the nc Ti powders range from 20 to 80 nm and the boundary width is approximated as 1.0 nm.[39] Exact boundary diffusion data for Ti at the studied temperatures is not available; however, a D_{gb}/D_v ratio from 2×10^3 to 1×10^4 is typical for alloys at temperatures below 0.75 T_{mp}.[39] This would suggest that the grain growth mechanism in nc Ti at lower temperatures is dominated by grain boundary diffusion, similar to what is observed in nc Cu.[31]

The stagnation of grain growth of the nc Ti samples after annealing at lower temperatures (150 °C to 350 °C) for extended periods of time may be attributed to the effects produced by solute/impurities drag, such as N atoms introduced during cryomilling. As the grain-boundary area decreases, the concentration of N atoms segregates to the boundaries, thus introducing a grain-size-dependent retarding force on the boundary migration. Similar experimental phenomena have been observed in other nc materials, including RuAl.[24]

C. *Recrystallization*

Annealing at higher temperatures (450 °C to 720 °C) led to recrystallization of the cryomilled nc Ti powders. The recrystallized fraction for each temperature was measured

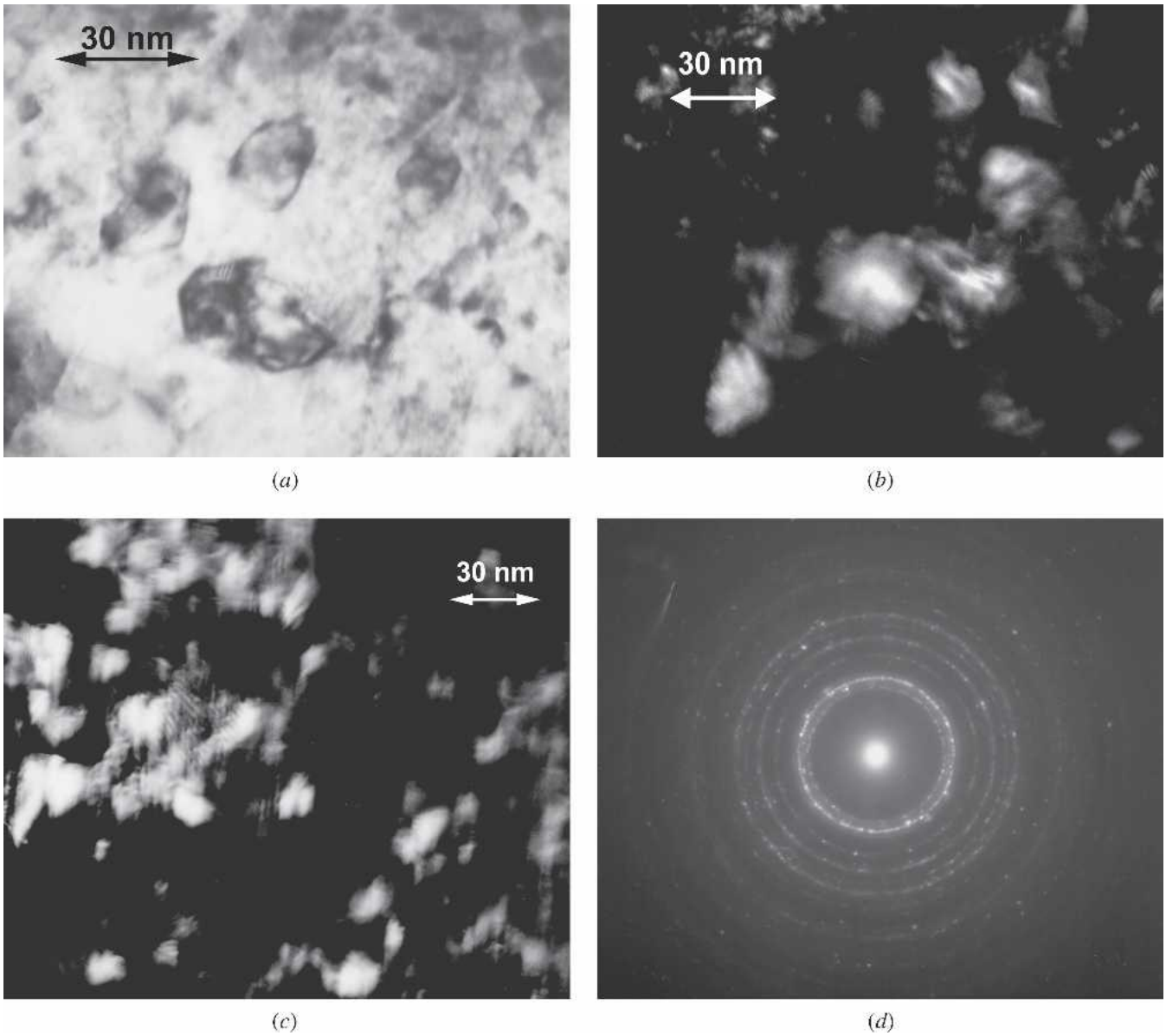

Fig. 3—(*a*) and (*b*) TEM bright-field and dark-field images of the 6h-cryomilled Ti powder, and (*c*) TEM DF image of the annealed Ti powder (675 °C for 60 min). (*d*) SADP corresponding to (c) showing that all SADP rings were attributed to the Ti matrix and no TiN existence was observed.

Table II. Grain Size Distribution (Number of Fraction, Percent) As-Cryomilled and As-Annealed at 675 °C for 60 Minutes

Grain Size, nm	1 to 15	16 to 25	26 to 35	36 to 45	>46
As-cryomilled	16.2	45.6	21.2	15.3	1.7
As-annealed	20.6	48.6	18.5	10.5	1.8

as a function of annealing time. In the present investigation, we do not measure the recrystallized fraction X_V directly, but intensities of the XRD peaks that are linearly related to the recrystallized fraction. This is so because a distinct shift of the XRD peaks was observed in recrystallized components compared to the original components. The integral intensities of the XRD peaks were calculated using Scintag XRD commercial software. The relation between X_V and the integral intensity I_R of recrystallized components and the integral intensity I_0 of the original components (non-recrystallized components) is as follows:

$$X_V = \frac{I_R}{I_R + I_0} \times 100 \text{ pct} \qquad [10]$$

In each experiment, the peak intensities of the six main peaks were employed to calculate the average recrystallized fraction X_V. For a quantitative evaluation, one should be aware of the fact that the time referred to as time zero is uncertain due to the heating rate. Therefore, the initiation of recrystallization cannot be determined with a high degree of accuracy.

Figure 6 shows the recrystallized fraction *vs* annealing time of the as-cryomilled nc Ti powder at different annealing temperatures (450 °C to 720 °C). As expected for diffusion-related phenomena, the rate of recrystallization increased

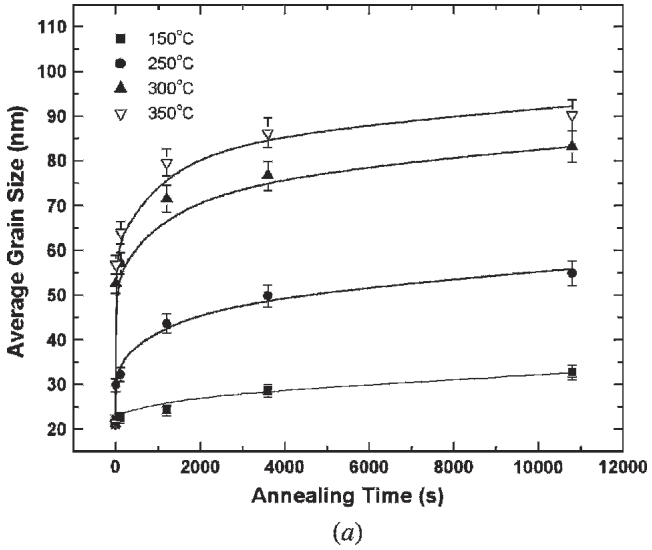

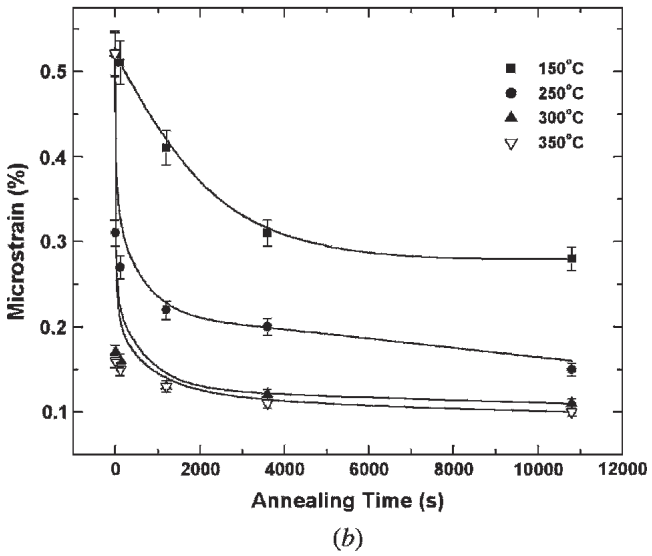

Fig. 4—(*a*) Grain size and (*b*) microstrain as a function of annealing time in the temperature range of 150 °C to 350 °C.

Table III. Parameters k and D_M Obtained by Fitting Equation [3]

Temperature (°C)	D_M (nm)	Rate Constant, k (nm^2/s)
150	33.6	0.120
250	63.1	0.533
300	83.2	2.260
350	98.2	3.320

with increasing annealing temperature. The kinetics of recrystallization has been commonly rationalized on the basis of the classic Johnson–Mehl–Avrami–Kolmogorov (JMAK) equation.[33]

$$X_V = 1 - \exp\left(-Bt^k\right) \qquad [11]$$

where X_V is the recrystallized fraction, t is the time, and B and k are constant. In Eq. [11], the constant B is the

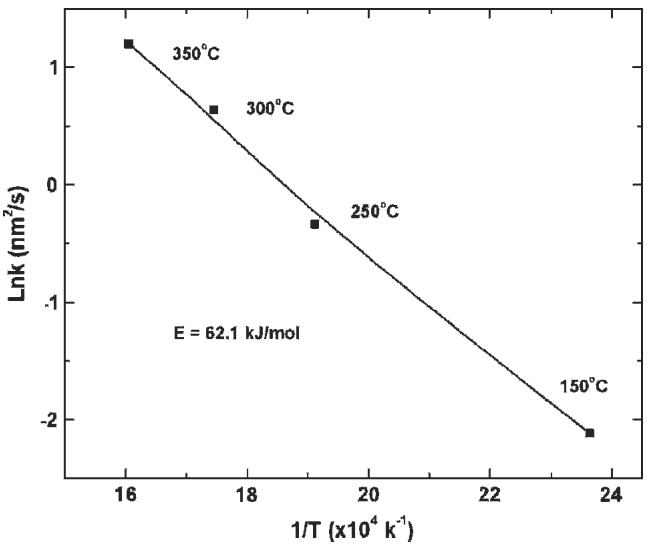

Fig. 5—Arrhenius plot of the parameter k (in Eq. [9]) *vs* the reciprocal annealing temperature.

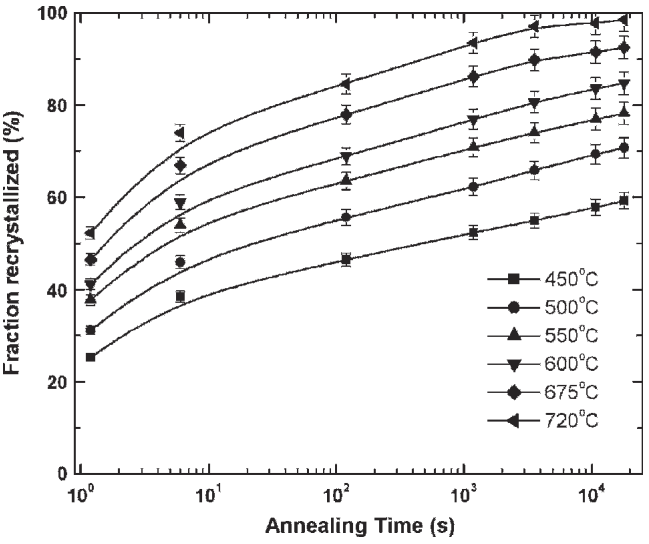

Fig. 6—Recrystallized fraction plotted *vs* annealing time.

temperature-dependent factor, which follows the Arrhenius equation. On the basis of the times required for 50 pct change in intensity, the activation energy for recrystallization has been determined to be 380.4 kJ/mol (Figure 7). This may be compared to the activation energy for recrystallization in cold-worked high-purity titanium, which has been reported as 304.6 kJ/mol.[39] The activation energy obtained from the data for 50 pct recrystallized fraction is unlikely to be constant, since it varies with changes in material purity, as it refers to the recrystallization process (nucleation and growth) as a whole.[23] By plotting ln $[(1/(1 - X_V))]$ *vs* ln t, as shown in Figure 8, values of $k = 0.142$ and $k = 0.105$ at 720 °C and 675 °C, respectively, were determined for the cryomilled nc Ti. These values and the resultant recrystallization kinetics will be discussed in detail in Section IV–B.

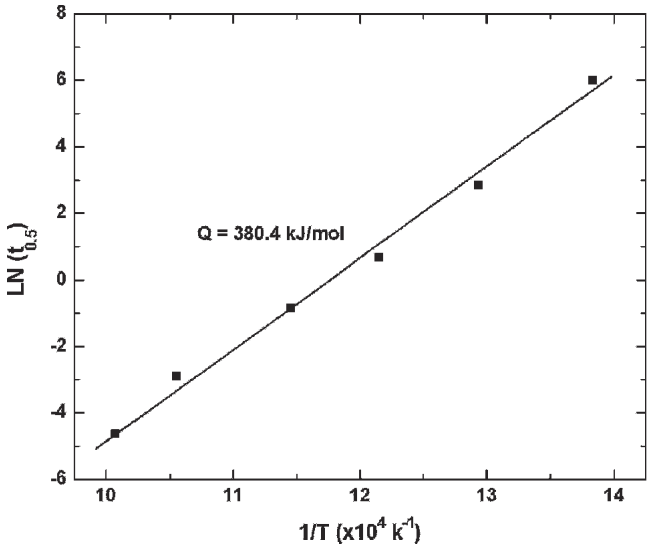

Fig. 7—Arrhenius plot of the time for 50 pct recrystallization as a function of temperature.

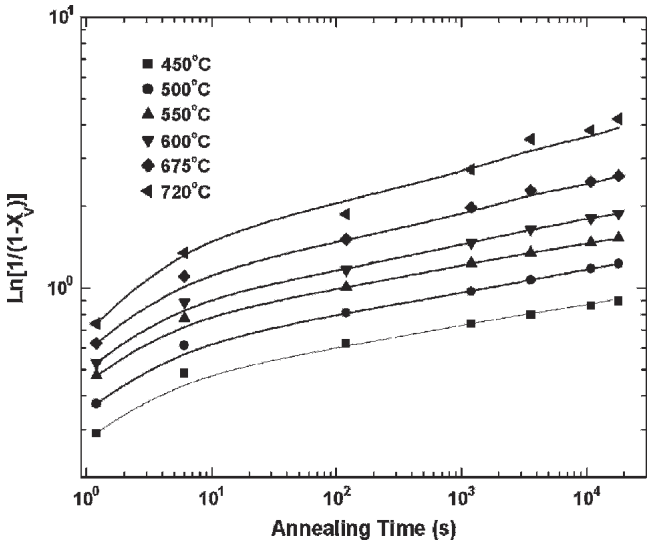

Fig. 8—JMA plot of the recrystallization kinetics of the cryomilled Ti powder.

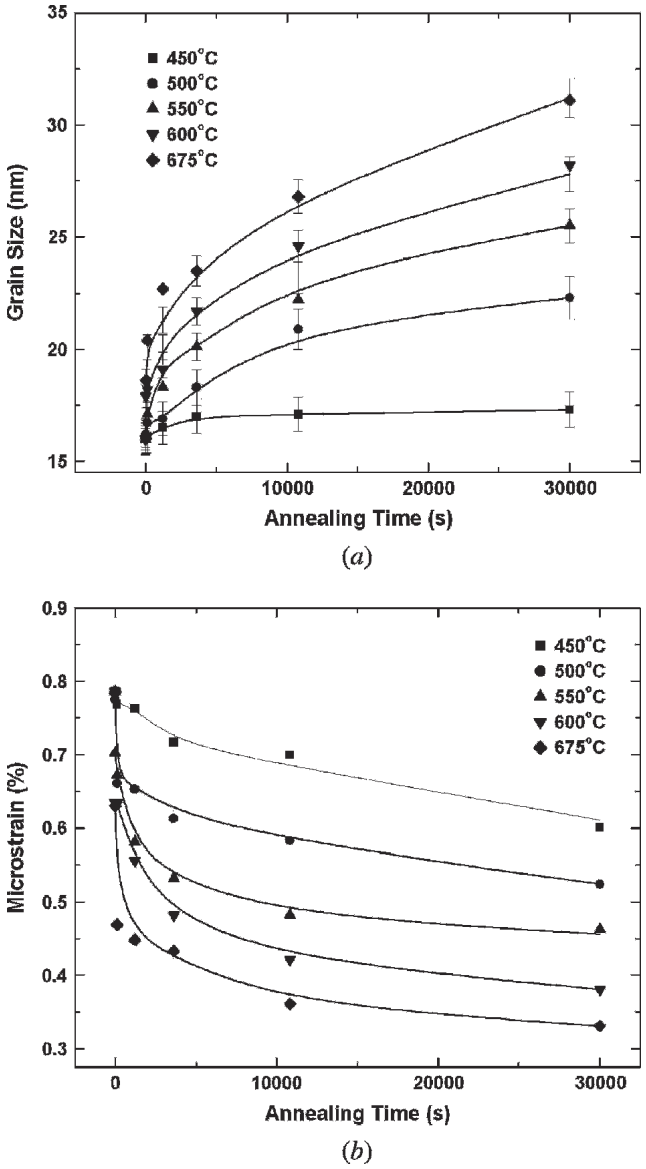

Fig. 9—(*a*) Grain size and (*b*) microstrain as a function of annealing time in the temperature range of 450 °C to 675 °C.

D. *Grain Growth at Elevated Temperatures (450 °C to 675 °C)*

Figure 9 shows the XRD measurement results of the variation of the average grain size and microstrain after each isothermal annealing in the temperature range of 450 °C to 675 °C for the cryomilled nc Ti samples. It can be seen that, with annealing time, the grain size increases and the microstrain decreases (both grain growth and microstrain release show temperature dependence). In addition, an examination of this figure reveals that the growth rate decreases with increasing annealing time (Figure 9(a)). The grain growth dependence on temperature can be fitted to an Arrhenius-type equation:[32]

$$D^n - D_0^n = k_0 t e^{-Q_G/RT} \qquad [12]$$

where D is the mean grain size after an annealing time t at a temperature T, D_0 the initial grain size, n the empirical time constant ($n \geq 2$), k_0 a constant, R the gas constant, and Q_G the activation energy for grain growth. The values of the empirical time exponent n were determined to be 10.9, 10.2, 9.78, and 9.32 for 500 °C, 550 °C, 600 °C, and 675 °C, respectively, as shown in Figure 10. Under ideal conditions, the time exponent n equals 2. For coarse polycrystalline Ti, the time exponent $n = 3$ was found to hold for the grain growth in pure Ti, Ti-7.4 Al, Ti-15.2 Mo, and Ti-11.5Mo-6Zr-4.5Sn alloys,[39–42] while $n = 5$ was observed in the two-phase Ti-6Al-4V alloy.[43] The time exponent has also been found to be higher than the theoretical value of 2 in many other grain growth experiments, and this is generally attributed to impediments that reduce the mobility of a grain boundary, such as dragging of solute atoms (N and O). Figure 11 shows the Arrhenius curves (Eq. [12]) for the

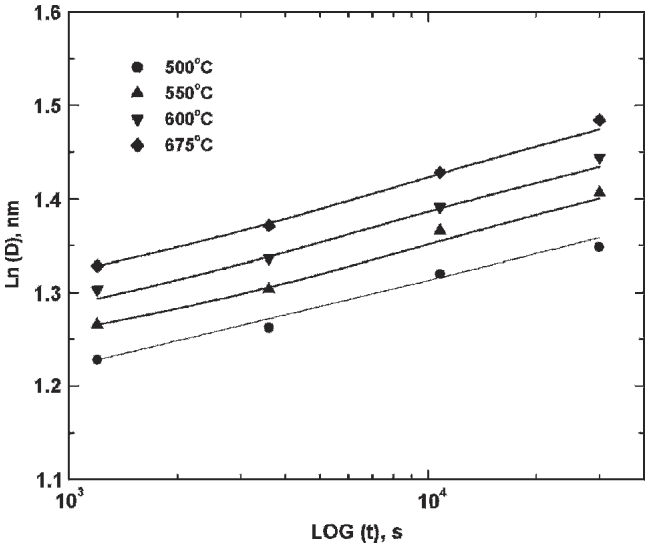

Fig. 10—Arrhenius plots for the time exponent n (Eq. [12]) in the temperature range of 500 °C to 675 °C.

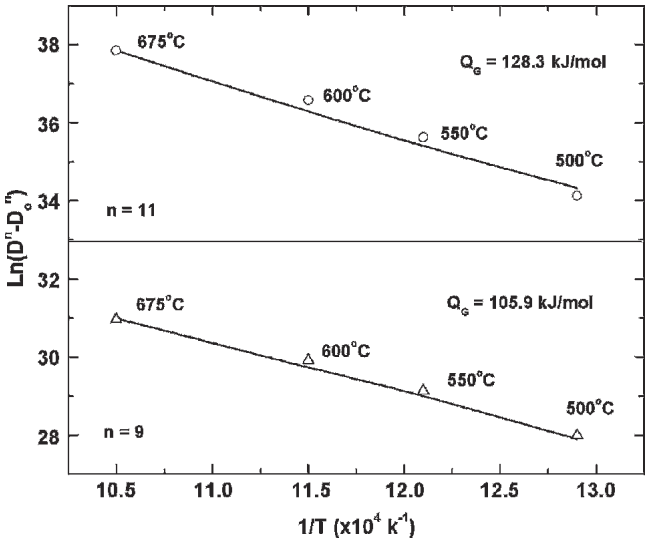

Fig. 11—Arrhenius plots for the grain growth of cryomilled Ti in the temperature range of 500 °C to 675 °C.

grain growth of cryomilled Ti for $n = 9$ and 11, respectively. The activation energies in the temperature range of 450 °C to 675 °C are 105.9 and 128.3 kJ/mol, respectively, and are lower than the activation energy for lattice self-diffusion of Ti (169.1 kJ/mol).[37]

IV. DISCUSSION

A. *Isochronal (Constant Annealing Time) Grain Growth Behavior*

The effect of the annealing temperature on the average grain size of the cryomilled nc Ti (Figure 2(a)) studied herein is different from that observed in other nc alloys such as Al, Zn, Fe, and Ni, reported in the literature.[8–13,23,29,30] The average grain size of the cryomilled Ti first increased in the temperature range of 200 °C to 350 °C, and then significantly decreased during annealing at 400 °C to 450 °C. This phenomenon is proposed to be associated with a recrystallization process in the cryomilled nc Ti powder.

There are three types of structural evolution during annealing: reordering, strain relaxation, and grain growth. During annealing in the lower temperature range (200 °C to 350 °C), grain growth and strain relaxation occur due to the fact that the driving force for grain growth is associated with a release of the lattice strain and the stored energy due to dislocations. The stored energy due to dislocations is given as[44]

$$E_D = \frac{G\mathbf{b}^2 f\rho}{4\pi}\ln\left(\frac{kR}{2\mathbf{b}}\right) \quad [13]$$

where E_D is the total strain energy, G the shear modulus, ρ the dislocation density, $\mathbf{b}$ the magnitude of Burgers vector, f a function of the Poisson's ratio, R the distance between the dislocations, and k the core energy factor (close to unity).[44]

Annealing at higher temperatures (400 °C to 450 °C) led to reordering of nitrogen atoms in hcp α-titanium. The reordering of nitrogen atoms present at octahedral interstices is associated with a decrease in chemical free energy in the cryomilled Ti, which is the primary driving force for the nucleation of recrystallized grains.[36] The amount of picked-up nitrogen in the cryomilled Ti powders is 2.01 wt pct, which is much higher than that in Ni, Al, and Zn.[8,9,10] Most of the nitrogen atoms in the cryomilled Ti are believed to be present in a solid-solution form, either in the interior of the grains or at the grain boundaries. This suggestion is motivated by two primary considerations. First, there was no evidence of nitride phases from the X-ray of TEM studies. Second, nitrogen is very soluble in hcp α-titanium by occupying the octahedral interstices: the maximum solubility of nitrogen is 8.9 wt pct. If one assumes a rigid spheres model, the radius of the octahedral interstice is 0.061 nm and the atomic radius of nitrogen is 0.068 nm.[36] A previous study[36] showed that the lattice parameters a and c in hcp α-titanium increased with nitrogen concentration. Our experimental results (Figure 1) show that the lattice parameters of recrystallized Ti are $a = 0.2959$ nm and $c = 0.4742$ nm, significantly larger than that of as-cryomilled nc Ti, indicating the reordering of nitrogen atoms in hcp α-titanium.

During recrystallization, the misfit between recrystallized grains and the matrix results in an elastic strain energy. In order to quantify the elastic strain energy due to coherency, it is generally assumed that the misfit between recrystallized grains and the matrix is purely dilatational and that the elastic properties of the recrystallized grains and the matrix are homogeneous and isotropic. Under these assumptions, the elastic strain energy G_E can be expressed by[45]

$$G_E = f(1-f)\frac{E}{1-v}\varepsilon^2 \upsilon^R \quad [14]$$

where E is the Young's modulus, ε the misfit parameter, υ^R the atomic molar volume of the recrystallized grains, and

f the volume fraction of the recrystallized grains. As shown in Figure 2(b), recrystallization led to a decrease in grain size and an increase in microstrain.

Recrystallization resulted in a smaller grain size of the recrystallized Ti, as shown in Figures 2(a) and 3. The grain size of recrystallized Ti is associated with both nucleation and growth processes that constitute recrystallization, which is different from the annealing behavior of the room-temperature milled Ti.[46] In the current study, the nucleation rate is thought to be much higher than the growth rate.

B. *Kinetics of Recrystallization*

Next, we should discuss the overall recrystallization kinetics, as shown in Figures 6 through 8 and as expressed in the classic JMA equation. The value of k is generally recognized to correspond with the shape of the recrystallized grains; usually the value lies between 1 and 2, but sometimes is less than 1.[32] The values of k observed in the current study were between 0.11 and 0.14, implying that the growth rate is not constant.

In previous investigations, the grain growth rate was found to decrease significantly with annealing time as follows:[32]

$$\dot{G} = Ct^{-r} \qquad [15]$$

where $\dot{G}$ is the growth rate, C a constant, t the annealing time, and r a parameter less than 1. When the variation of the growth rate with time is given by Eq. [15], the JMA equation may be modified as[32]

$$X_v = 1 - \exp\left[-fN\left(C\frac{t^{(1-r)}}{1-r}\right)^3\right] \qquad [16]$$

Note that with increasing r, the grain growth rate slowly decreases, thus leading to slower recrystallization kinetics.

Figure 6 shows the short incubation period and low rate of overall recrystallization in cryomilled Ti. On one hand, this observation may be attributed to easier nucleation on the densely distributed grain boundaries of the cryomilled Ti. On the other hand, the low rate of overall recrystallization might be attributed to the intrinsically higher elastic strain energy between recrystallized grains and the matrix due to misfit, and the lower mobility of grain boundaries. During recrystallization, a growing recrystallized grain is acted on by opposing pressure arising from the elastic strain energy between recrystallized grains and the matrix. In addition, it is known that the presence of solute atoms drastically reduces the mobility of a grain boundary *via* the formation of a solute atmosphere near the grain boundaries. It appears likely, therefore, that the recrystallization of cryomilled nc Ti is controlled by the diffusivity of solute atoms, *i.e.,* nitrogen atoms in the Ti matrix.

C. *Increased Thermal Stability*

It is important to understand the mechanisms that govern the thermal stability of nc materials for the reasons outlined earlier. Previous investigations[8–13] indicated that the thermal stability of nc Al, Zn, Fe, and Ni could be improved by introducing oxides or nitrides. However, the variation of grain size in these nc materials showed a positive temperature dependence in a wide range of annealing temperatures.

It is therefore of scientific and technological significance in finding that a smaller grain size can be obtained in cryomilled nc Ti at a higher annealing temperature through a recrystallization process. Based on this finding, a new class of nc materials could be designed and synthesized, and their thermal stability could be further enhanced through the recrystallization process. This type of nc materials is expected to be observed in many mechanically milled M-X alloy systems (M = Ti, Al, Ni, or Fe; X = C, N, or B), where diffusion-induced recrystallization occurs at higher temperatures.

V. CONCLUSIONS

In this article, an nc Ti alloy was produced by a cryomilling technique. The grain growth, thermal stability, and recrystallization behavior have been investigated in a temperature range of 150 °C to 720 °C. The primary results are briefly summarized as follows.

1. In the temperature range from 200 °C to 350 °C, an increase in the average grain size was observed from 20 to 80 nm. With a further increase of the annealing temperature, a significant drop of the average grain size (to about 15 nm) was observed during annealing at 400 °C to 450 °C, which resulted from a recrystallization process. When the annealing temperature increased from 450 °C to 720 °C, the grain size increased from 15 to 28 nm, indicating that no significant grain growth occurs between 450 °C and 720 °C.
2. At lower temperatures (150 °C to 350 °C), grain growth stagnated after a certain annealing time, while microstrain decreased rapidly. The stagnation of grain growth may be attributed to the effects of solute/impurities drag, such as N atoms introduced during cryomilling. As the grain-boundary area decreases, the N atoms segregated to the boundaries, thus introducing a grain-size-dependent retarding force on the boundary migration.
3. Recrystallization occurred when annealing above 450 °C due to the reordering of nitrogen atoms in octahedral interstices in α-Ti phase. The recrystallization rate obeyed the JMA equation. The time exponent k was less than unity and increased with increasing temperature. The low rate of overall recrystallization is attributed to the intrinsically higher elastic strain energy between recrystallized grains and the matrix due to misfit, and the lower mobility of grain boundaries.
4. In the temperature range of 450 °C to 675 °C, the grain growth obeyed the expression $D^n - D_0^n = k_0 t e^{-Q_G/RT}$, where D is the grain diameter. The time exponent n was found to be 9.3 to 10.9, much higher than the theoretical value of 2, and this is attributed to impediments acting on the moving grain boundary, such as solute drag (N and O).

ACKNOWLEDGMENT

The authors acknowledge the financial support provided by the Office of Naval Research (Grant No. N00014-04-1-0370).

REFERENCES

1. H. Gleiter: *Acta Mater.*, 2000, vol. 48, pp. 1-29.
2. K.S. Kumar, H. Van Swygenhoven, and S. Suresh: *Acta Mater.*, 2003, vol. 51, pp. 5743-74.
3. C.C. Koch: *Nanostr. Mater*, 1997, vol. 9, pp. 13-22.
4. H.J. Fecht: *Nanostr. Mater*, 1995, vol. 6, pp. 33-42.
5. R. Birringer: *Mater. Sci. Eng.*, 1989, vol. A117, pp. 33-43.
6. R. Günter, A. Kumpmann, and H.D. Kunze: *Scripta Metall. Mater.*, 1992, vol. 27, pp. 833-38.
7. J. Weissmüller, J. Löffler, and M. Kleber: *Nanostr. Mater*, 1995, vol. 6, pp. 105-14.
8. J. He and E.J. Lavernia: *J. Mater. Res.*, 2001, vol. 16, pp. 2724-32.
9. F. Zhou, S.R. Nutt, C.C. Bampton, and E.J. Lavernia: *Metall. Mater. Trans. A*, 2003, vol. 34A, pp. 1985-92.
10. Y. Xun, E.J. Lavernia, and F.A. Mohamed: *Metall. Mater. Trans. A*, 2004, vol. 35A, pp. 573-81.
11. V.L. Tellkamp, A. Melmed, and E.J. Lavernia: *Metall. Mater. Trans. A*, 2004, vol. 35A, pp. 2335-43.
12. V.L. Tellkamp, S. Dallek, D. Cheng, and E.J. Lavernia: *J. Mater. Res.*, 2001, vol. 16 (4), pp. 938-44.
13. B. Huang, R.J. Perez, and E.J. Lavernia: *Mater. Sci. Eng.*, 1998, vol. A255, pp. 124-32.
14. J. Ecker, J.C. Holzer, and W.L. Johnson: *J. Appl. Phys.*, 1993, vol. 73, pp. 131-35.
15. R. Abe, J.C. Holzer, and W.L. Johnson: *Mater. Res. Soc. Symp. Proc.*, 1992, vol. 238, pp. 721-27.
16. C.E. Krill, R. Klein, S. Janes, and R. Birringer: *Mater. Sci. Forum*, 1995, vols. 179–181, pp. 443-49.
17. P. Knauth, A. Charai, and P. Gas: *Scripta Metall. Mater.*, 1993, vol. 28, pp. 325-30.
18. A. Kumpmann, R. Günter, and H.D. Kunze: *Mater. Sci. Eng.*, 1993, vol. A168, pp. 165-69.
19. K. Boylan, D. Ostrander, U. Erb, G. Palumbo, and K.T. Aust: *Scripta Metall. Mater.*, 1991, vol. 25, pp. 2711-16.
20. H.J. Höfler and R.S. Averback: *Scripta Metall. Mater.*, 1990, vol. 24, pp. 2401-06.
21. Z. Gao and B. Fultz: *Nanostr. Mater*, 1994, vol. 4, pp. 939-47.
22. C. Bansal, Z. Gao, and B. Fultz: *Nanostr. Mater*, 1995, vol. 5, pp. 327-36.
23. T.R. Malow and C.C. Koch: *Acta Mater.*, 1997, vol. 45, pp. 2177-86.
24. K.W. Liu and F. Müchlich: *Acta Mater.*, 2001, vol. 49, pp. 395-403.
25. L. He and E. Ma: *Nanostr. Mater*, 1996, vol. 7, pp. 327-39.
26. P.A. Beck, J.C. Kremer, L.J. Demer, and M.L. Holzworth: *Trans. Am. Inst. Min. Eng.*, 1948, vol. 175, pp. 372-76.
27. J.E. Burke: *Trans. Am. Inst. Min. Eng.*, 1949, vol. 180, pp. 73-77.
28. A. Michels, C.E. Krill, H. Ehrhardt, R. Birringer, and D.T. Wu: *Acta Mater.*, 1999, vol. 47, pp. 2143-52.
29. F. Zhou, X.Z. Liao, Y.T. Zhu, S. Dallek, and E.J. Lavernia: *Acta Mater.*, 2003, vol. 51, pp. 2777-91.
30. J. Lee, F. Zhou, K.H. Chung, N.J. Kim, and E.J. Lavernia: *Metall. Mater. Trans. A*, 2001, vol. 32A, pp. 3109-15.
31. L. Lu, N.R. Tao, and L. Wang: *J. Appl. Phys.*, 2001, vol. 89, pp. 6408-12.
32. F.J. Humphreys and M. Hatherly: *Recrystallization and Related Annealing Phenomena,* Pergamon Press, Oxford, United Kingdom, 1996.
33. T.H. De Keijser, J.I. Langford, E.J. Mittemeijer, and A.B.P. Vogels: *J. Appl. Crystallogr.*, 1982, vol. 15, pp. 308-12.
34. K.H. Chung and E.J. Lavernia: *Metall. Mater. Trans. A*, 2002, vol. 33A, pp. 3795-801.
35. F. Zhou, D. Witkin, S. R. Nutt, and E.J. Lavernia: *Mater. Sci. Eng.,* 2004, vols. A375–A377, pp. 917-21.
36. D. David, E.A. Garcia, and G. Beranger: in *Titanium '80 Science and Technology,* H. Kimura and O. Izumi, eds., American Institute of Mining, Metallurgical, and Petroleum Engineers, Inc., Warrendale, PA, 1980, pp. 537-43.
37. E.A. Brandes and G.B. Brook: *Smithels Metals Reference Book*, 7th ed., Butterworth-Hernemann Ltd., Oxford, United Kingdom, 1992, pp. 13-11-13-118.
38. D.A. Porter and K.E. Easterling: *Phase Transformations in Metals and Alloys,* Van Nostrand Reinhold, Workingham, United Kingdom, 1988, pp. 101-02.
39. H. Hu and R.S. Cline: *Trans. TMS-AIME*, 1968, vol. 242, pp. 1013-24.
40. B.B. Rath, R.J. Lederich, C.F. Yolton, and F.H. Froes: *Metall. Trans. A*, 1979, vol. 10A, pp. 1013-19.
41. P. Ganesan, K. Okazaki, and H. Conrad: *Metall. Trans. A*, 1979, vol. 10A, pp. 1021-29.
42. H. Hu and B.B. Rath: *Metall. Trans. A*, 1970, vol. 1A, pp. 3181-84.
43. C.H. Johnson, S.K. Richter, C.H. Hamilton, and J.J. Hoyt: *Acta Mater.*, 1999, vol. 47, pp. 23-29.
44. J.P. Hirth and J. Lothe: *Theory of Dislocations,* 2nd ed., Wiley, New York, NY, 1982.
45. J.W. Cahn and F.C. Larche: *Acta Metall.*, 1984, vol. 32, pp. 1915-23.
46. T.D. Shen and C.C. Koch: *Nanostr. Mater*, 1995, vol. 5, pp. 615-29.